Atmospheric Environment 262 (2021) 118630

Contents lists available at ScienceDirect

Atmospheric Environment

journal homepage: www.elsevier.com/locate/atmosenv

Characterization and ozone formation potential (OFP) of non-methane hydrocarbons under the condition of chemical loss in Guangzhou, China

Y. Zou [a,*], E. Charlesworth [b], N. Wang [a,**], R.M. Flores [c], Q.Q. Liu [a], F. Li [d], T. Deng [a], X.J. Deng [a]

[a] Institute of Tropical and Marine Meteorology, China Meteorological Administration (CMA), Guangzhou, China
[b] IEK-7 Stratosphere, Research Center Jülich, Germany
[c] Marmara University, Department of Environmental Engineering, Istanbul, Turkey
[d] Xiamen Key Laboratory of Straits Meteorology, China

HIGHLIGHTS

- Characterization and OFP of NMHCs were obtained in Guangzhou under the condition of chemical loss.
- The initial daytime mixing ratios were approximately 6.00 ppbv higher than the observed.
- The OFP of NMHCs chemical loss was calculated by four versions of MIR.
- Vehicle exhaust emissions and solvent use were the important sources of NMHCs in Guangzhou.

GRAPHICAL ABSTRACT

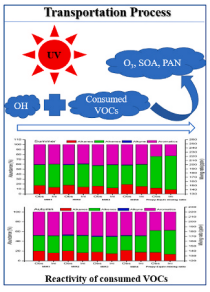

ARTICLE INFO

Keywords:
NMHCs
Photochemical pollution
MIR
PMF
Megacity

ABSTRACT

The conventional analytical studies to determine ozone formation potential (OFP) and potential sources currently ignore the destruction of non-methane hydrocarbons (NMHCs) during atmospheric transport, namely chemical loss. The chemical loss of NMHCs was estimated using photochemical age based on the online observation data of NMHCs from the Guangzhou Panyu Atmospheric Composition Station (GPACS) in the Pearl River Delta (PRD) during summer (June, July, and August) and autumn (September, October, and November) - two seasons favorable to the photochemical generation of ozone - of 2012. Subsequently, the composition characteristics, OFPs, and potential sources of the NMHCs were analyzed under the condition of atmospheric photochemical loss. The results showed that the initial mixing ratios of NMHCs (i.e., the mixing ratios after discharge from emission sources, before they experience any significant atmospheric chemical reaction), during summer (37.30 ppbv) and autumn (41.62 ppbv) were 6.90 ppbv and 5.98 ppbv higher than the observed, respectively. Four maximum incremental reactivity (MIR) scales were used to calculate the OFP for NMHCs seasonal losses. The obtained OFPs were 62.67 ppbv, 73.05 ppbv, 73.31 ppbv, and 68.51 ppbv in summer and 47.71 ppbv, 55.54 ppbv, 56.12 ppbv, and 52.68 ppbv in autumn as calculated by the respective MIR scales. Both the MIR and the

* Corresponding author.
** Corresponding author.
E-mail addresses: yzou@gd121.cn (Y. Zou), wangn@gd121.cn (N. Wang).

https://doi.org/10.1016/j.atmosenv.2021.118630
Received 26 February 2021; Received in revised form 7 July 2021; Accepted 17 July 2021
Available online 23 July 2021

propylene-equivalent mixing ratio reflect the reactivity of various NMHC species to a certain extent. Isoprene, toluene, and xylene were found key species for controlling ozone. Based on the source analysis of the initial mixing ratio of NMHCs, vehicle emissions and solvent consumption were the major sources in Guangzhou.

1. Introduction

With economic development, the long-term strong emissions of atmospheric pollutants in the Pearl River Delta (PRD) have caused combined pollution that has become increasingly prominent in this region. The problem of air quality in this region has gradually changed from $PM_{2.5}$-dominated haze pollution to ozone-dominated photochemical pollution (Wang et al., 2009; Zheng et al., 2010; Ling et al., 2017). Atmospheric volatile organic compounds (VOCs) are important precursors of secondary pollutants in the atmosphere. The photochemical ozone formation in urban areas of Hong Kong and the inland PRD region is dominated by VOCs (Zhang et al., 2008a; Ou et al., 2016; Guo et al., 2017; Wang et al., 2019). In the past few decades, many studies have been carried out on the mixing ratio levels of VOCs, their atmospheric chemical reactivities, their sources, and their nonlinear relationships with ozone formation in the region (e.g., Shao et al., 2000; Zheng et al., 2009; Cheng et al., 2010; Guo et al., 2017; Zou et al., 2015; Zou et al., 2019a). During transport, photochemical loss (i.e., destruction) of VOCs and ozone production occur simultaneously. However, this ozone production can't be measured by conventional means. Therefore, the conventional analytical studies in urban regions inevitably have run into problems as they determine photochemical ozone formation potential (OFP) and potential sources based on locally measured atmospheric VOC mixing ratios. For example, Xie et al., (2008) found that the atmospheric chemical loss of VOCs in the transport process accounted for 1/3 of the OFP in the urban area of Beijing. Na and Kim (2007) and Bon et al., (2011) used the chemical mass balance (CMB) and positive matrix factorization (PMF) receptor models, respectively, to analyze VOC sources and found that neglecting chemical loss during VOC transport resulted in underestimated source contribution. Therefore, it is of great significance to evaluate the chemical loss of VOCs in the atmosphere.

There are two common methods for estimating the chemical loss of VOCs in the atmosphere. One is to select species pairs of VOCs with the same origin but different reactivities and obtain their chemical loss using photochemical age (Mckeen et al., 1996); the other method is to calculate the chemical loss of VOCs by measuring the oxidation products of VOCs (Wiedinmeyer et al., 2001). Although studies(Shao et al., 2011; Shiu et al., 2007; Wang et al., 2013) have investigated the chemical loss of atmospheric VOCs in various regions of China (such as Beijing, Shanghai, and Taiwan), relatively few studies have focused on Guangzhou in the PRD.

The chemical loss of the non-methane hydrocarbons (NMHCs) - one class of VOCs - was estimated by using photochemical age based on the online observation data of NMHCs from the Guangzhou Panyu Atmospheric Composition Station (GPACS) in the PRD. The measurements were performed during summer (June, July, and August) and autumn (September, October, and November) - two seasons favorable to the photochemical generation of ozone - of 2012. Subsequently, the composition characteristics, OFP, and potential sources of the NMHCs were analyzed under the condition of atmospheric photochemical loss to provide a guideline for the comprehensive management of atmospheric photochemical ozone formation in Guangzhou.

2. Methodology

2.1. Site description

NMHCs and ozone were measured simultaneously at the Guangzhou Panyu Atmospheric Composition Station (GPACS) operated by the Institute of Tropical and Marine Meteorology (ITMM) of the China Meteorological Administration (CMA). The GPACS site (23.00 N, 113.35 E, 141 m.a.g.l), located at the center of the PRD on the hilltop of Dazhengang, Nancun Town, Panyu District, Guangzhou, China (Fig. 1), is the main station for atmospheric composition observation network of Guangdong Meteorological Bureau. It is approximately 120 m above the city and surrounded by residential neighborhoods with no significant industrial pollution sources nearby (Tan et al., 2016; Liu et al., 2018). Fig. 2 shows that the relative contributions of the four categories of NMHCs (i.e., alkanes, alkenes, alkynes, and aromatics) in summer and autumn remained fairly uniformity regardless of the large variation in their mixing ratios. Such uniformity implies that the air at GPACS was sufficiently homogeneous with regards to various sources near the surface, which has also been confirmed by previous studies (Zou et al., 2015, 2019a). For this reason, this site was chosen for NMHCs photochemical loss in this study.

2.2. Instrumentation

NMHCs were measured using the GC5000 analysis systems from AMA Instruments GmbH, Germany. The system consists of two sets of sampling systems and two sets of chromatography column systems, including a low boiling point VOC analyzer for C_2–C_6 NMHCs species and a high boiling point BTX analyzer for C_6–C_{12} NMHCs species. The Photochemical Assessment Monitoring Stations (PAMS) standard gas approved by the U.S. EPA was used to calibrate the NMHCs species during the monitoring period, and the retention time and system response were adjusted to maintain the calibration. The NMHCs data validation program was recommended by the U.S. EPA PAMS (i.e., species which exceeded 20% of the total NMHCs or were 3 sigma above the mean of that species were flagged as an outlier if no explanation could be found after further inspection) (Main et al., 1999). During the observation period, it was found that benzene mixing ratios were abnormally high due to a disturbance by a water peak. Therefore, the benzene mixing ratios were not considered in this study. The outliers (~10%) were eliminated before data processing to ensure the quality of the analysis. The method detection limits (MDL) and the linear correlation coefficients of the calibration curve (R^2) are shown in Table 1. Ozone was measured by an EC9810B ozone analyzer (Ecotech Co., Australia) based on the UV-absorption method and the Lambert-Beer law (Zou et al., 2019a).

Fig. 1. Observation site and its surrounding area in Guangzhou (Source: Google Maps).

2.3. Data analysis

2.3.1. Estimation of the initial mixing ratio of NMHCs

After NMHCs are discharged from emission sources, photochemical loss occurs during their subsequent transport. NMHCs are eventually observed at monitoring stations. The initial mixing ratio of NMHCs is the mixing ratio of NMHCs after discharge from emission sources but before they experience any significant atmospheric chemical reaction. The observed mixing ratio is the mixing ratio of NMHCs observed at the monitoring site. The chemical loss during transport of NMHCs is the difference between the initial mixing ratio and the observed mixing ratio.

At present, the methods for estimating the chemical loss of NMHCs in the atmosphere can be divided into two broad categories. One category estimates NMHCs loss through reaction kinetics based on the measurements of the known oxidation products of NMHC species. For example, Xie et al., (2008) estimated the initial NMHC mixing ratio using the observation data of isoprene and its oxidation products (e.g., methyl vinyl ketone (MVK) and methacrolein (MACR)). This approach requires the simultaneous measurements of isoprene, MVK, and MACR. And the approach is only valid during daytime. Another category of methods uses a photochemical age-based method to estimate the chemical loss of NMHCs (McKeen et al., 1996), which was the method used in this work because the measurement of the oxidation products of NMHCs is not necessary. In this method, the air mass aging is represented by a group of specific pairs of NMHC species with the same origin but different chemical reactivities (Wang et al., 2013; Gao et al., 2018).

Using this method, the formula to calculate the initial mixing ratio of NMHCs is as follows:

$$[NMHC_i]_t = [NMHC_i]_0 \times \exp(-K_i[OH]\Delta t) \quad (1)$$

$$\Delta t = \frac{1}{[OH](k_C - k_B)} \times \left(\ln\left\{\frac{[C]}{[B]}\middle| t = t_0\right\} - \ln\left\{\frac{[C]}{[B]}\middle| t = t\right\}\right) \quad (2)$$

where $[NMHC_i]_t$ is the mixing ratio of $NMHC_i$ at the observation site, $[NMHC_i]_0$ is the initial $NMHC_i$ mixing ratio discharged from its emission sources, B and C are a pair of specific NMHC species, K_i is the rate constant for the reaction of OH radical with $NMHC_i$ (Atkinson and Arey, 2003), k_B is the rate constant for the reaction of OH radical with $NMHC_B$, k_C is the rate constant for the reaction of OH radical with $NMHC_C$ (Table 2), [OH] is the mixing ratio of OH radicals, Δt is the photochemical age of air mass, $\left(\frac{[C]}{[B]}\right)t = t_0$ is the ratio of the initial emission mixing ratio of $NMHC_C$ to the initial emission mixing ratio of $NMHC_B$, and $\left(\frac{[C]}{[B]}\right)\ t = t$ is the ratio of the observed emission mixing ratio of $NMHC_C$ to the observed emission mixing ratio of $NMHC_B$ at time t.

The following assumptions were made when this estimation method was adopted:

(1) All major NMHC species are discharged from the same source (Mckeen et al., 1996). Although this assumption does not reflect the variation in emission sources observed in reality, it has been widely used in other studies (Gao et al., 2018; Wang et al., 2013; Zhan et al., 2021) and has been proven acceptable.

(2) The emissions of major NMHC species are fixed, and the influence of fresh emission sources during transport is negligible (Bertman et al., 1995). As described in Section 2.1, the air at GPACS was sufficiently homogeneous with regards to various sources near the surface, which

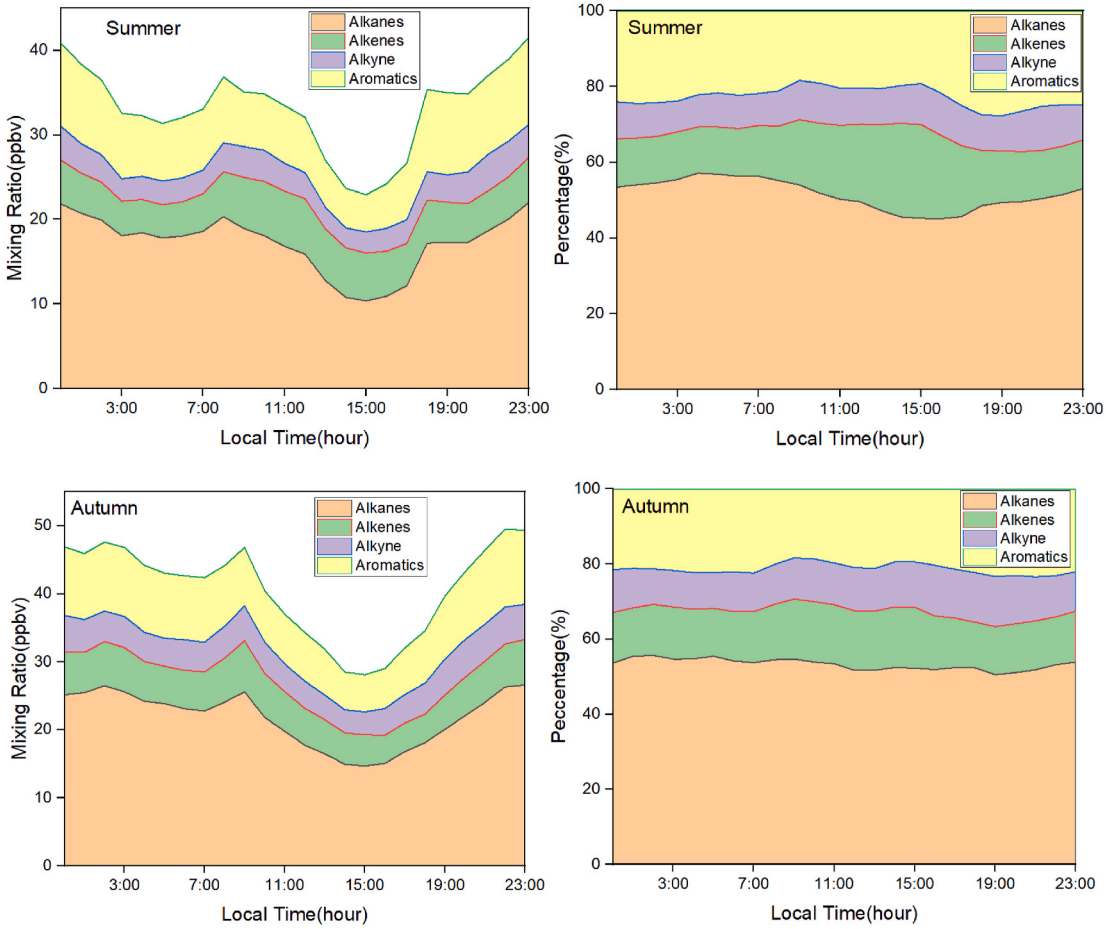

Fig. 2. Diurnal variation of hourly averaged mixing ratios (ppbv) of four categories of NMHCs and relative abundance (%) in summer and autumn at GPACS.

Table 1
Method detection limits and linear correlation coefficient of the 55 target species.

Compound	MDL (ppbv)	R^2
Alkanes		
Ethane	0.08	0.997
Propane	0.09	0.998
i-Butane	0.05	0.994
n-Butant	0.05	0.994
Cyclopentane	0.06	0.997
i-Pentane	0.07	0.998
n-Pentane	0.07	0.984
Mehtylcyclopentane	0.07	0.999
2,3-Dimethylbutane	0.07	0.999
2-Methylpentane	0.07	0.994
3- Methylpentane	0.07	0.998
n-Hexane	0.06	0.997
2,4-Dimethylpentane	0.05	0.999
2,2-Dimethylbutane	0.07	0.998
Cyclohexane	0.07	0.997
2-Methylhexane	0.04	0.990
2,3-Dimethylpentane	0.05	0.997
3-Methylhexane	0.04	0.991
2,2,4-Trimethylpentane	0.05	0.994
n-Heptane	0.05	0.994
Methylcyclohexane	0.05	0.995
2,3,4-Trimethylpentane	0.04	0.994
2-Methylheptane	0.04	0.990
3-Methylheptane	0.04	0.991
n-Octane	0.04	0.989
n-Nonane	0.06	0.997
n-Decane	0.04	0.995
n-Undecane	0.04	0.992
n-Dodecane	0.05	0.993
Alkenes+Alkyne		
Ethene	0.07	0.997
Propene	0.07	0.999
trans-2-Butene	0.05	0.997
1-Butene	0.06	0.994
cis-2-Butene	0.06	0.999
trans-2-Pentene	0.07	0.998
1-Pentene	0.05	0.998
cis-2-Pentene	0.07	0.984
Isoprene	0.07	0.998
1-Hexene	0.05	0.995
Acetylene	0.05	0.996
Aromatics		
Toluene	0.05	0.995
Ethylbenzene	0.04	0.992
m,p-Xylene	0.03	0.994
Styrene	0.04	0.991
o-Xylene	0.04	0.989
i-Propylbenzene	0.04	0.986
n-Propylbenzene	0.04	0.986
p-Ethyltoluene	0.04	0.989
m-Ethyltoluene	0.04	0.989
1,3,5-Trimethylbenzene	0.04	0.989
o- Ethyltoluene	0.04	0.999
1,2,4-Trimethylbenzene	0.03	0.991
1,2,3-Trimethylbenzene	0.04	0.993
m-Diethylbenzene	0.04	0.991
p-Diethylbenzene	0.04	0.993

MDL: method detection limit.
R^2: linear correlation coefficient of the calibration curve.

indicated that this assumption was applicable for estimation of initial NMHCs mixing ratios at GPACS in Guangzhou. We assumed that the average [OH] was 5×10^6 molecules/cm^3, the mean photochemical age of air mass estimated was 1.41 h, most of the NMHCs ages were <3 h, long-range transport from other regions could be excluded in this study. It should be noted that uncertainty in the initial mixing ratios would increase when atmospheric turbulence was severe (Parrish et al., 2007).

(3) Chemical loss of NMHCs during transport is only caused by their

Table 2
MIR factor scales and reaction rate constants (*K*) of used in this study.

Compound	MIR1	MIR2	MIR3	MIR4	$K^a \times 10^{12}$
Alkanes					
Ethane	0.25	0.31	0.28	0.32	0.27
Propane	0.48	0.56	0.49	0.56	1.15
i-Butane	1.21	1.35	1.23	1.30	2.34
n-Butant	1.02	1.33	1.15	1.33	2.54
Cyclopentane	2.4	2.69	2.39	2.37	5.16
i-Pentane	1.38	1.68	1.45	1.65	3.90
n-Pentane	1.04	1.54	1.31	1.56	3.94
Mehtylcyclopentane	2.8	2.42	2.19	2.23	5.10
2,3-Dimethylbutane	1.07	1.14	0.97	1.09	6.30
2-Methylpentane	1.5	1.8	1.5	1.77	5.60
3- Methylpentane	1.5	2.07	1.8	2.09	5.70
n-Hexane	0.98	1.45	1.24	1.55	5.60
2,4-Dimethylpentane	1.5	1.65	1.55	1.76	5.70
2,2-Dimethylbutane	NA	1.33	1.17	1.30	2.32
Cyclohexane	1.28	1.46	1.25	1.81	7.49
2-Methylhexane	1.08	1.37	1.19	1.57	6.90
2,3-Dimethylpentane	1.31	1.55	1.34	1.55	5.10
3-Methylhexane	1.40	1.86	1.61	1.91	5.10
2,2,4-Trimethylpentane	0.93	1.44	1.26	1.38	3.68
n-Heptane	0.81	1.28	1.07	1.37	7.15
Methylcyclohexane	1.80	1.99	1.70	1.86	10.4
2,3,4-Trimethylpentane	1.60	1.23	1.03	1.20	7.00
2-Methylheptane	0.96	1.20	1.07	1.37	8.30
3-Methylheptane	0.99	1.35	1.24	1.53	8.60
n-Octane	0.60	1.11	0.90	1.15	8.68
n-Nonane	0.54	0.95	0.78	1.03	10.20
n-Decane	0.46	0.83	0.68	0.93	11.60
n-Undecane	0.42	0.74	0.61	0.85	13.20
n-Dodecane	0.38	0.66	0.55	0.79	14.20
Alkenes+Alkyne					
Ethene	7.40	9.08	9.00	8.64	8.50
Propene	9.40	11.58	11.66	10.80	26.30
trans-2-Butene	10.00	13.91	15.16	12.50	64.00
1-Butene	8.90	10.29	9.73	9.30	31.40
cis-2-Butene	10.00	13.22	14.24	12.20	56.40
trans-2-Pentene	8.80	10.23	10.56	9.74	67.00
1-Pentene	6.20	7.79	7.21	6.92	31.40
cis-2-Pentene	8.80	10.24	10.38	9.62	65.00
Isoprene	9.10	10.69	10.61	9.71	101.00
1-Hexene	4.40	6.17	5.49	5.47	NA
Acetylene	0.50	1.25	0.95	0.94	0.83
Aromatics					
Toluene	2.70	3.90	4.00	4.02	5.96
Benzene	0.42	0.81	0.72	0.79	1.23
Ethylbenzene	2.70	2.79	3.04	3.11	6.96
m,p-Xylene	7.40	7.43	7.80	6.99	20.50
Styrene	2.20	1.95	1.73	1.70	58.0
o-Xylene	6.50	7.49	7.64	7.17	13.6
i-Propylbenzene	2.20	2.32	2.52	2.58	6.60
n-Propylbenzene	2.10	2.20	2.03	2.15	5.70
p-Ethyltoluene	NA	3.75	4.44	4.28	18.60
m-Ethyltoluene	NA	9.37	7.39	6.70	11.80
1,3,5-Trimethylbenzene	10.10	11.22	11.76	9.35	56.7
o- Ethyltoluene	NA	6.61	5.59	5.33	11.90
1,2,4-Trimethylbenzene	8.80	7.18	8.87	7.88	32.50
1,2,3-Trimethylbenzene	8.90	11.26	11.97	9.86	32.70
m-Diethylbenzene	NA	8.39	7.10	6.30	15.00
p-Diethylbenzene	NA	3.36	4.43	4.18	10.00

1) "NA"denotes MIR values were not enlisted in the literature.
2) MIR1 denotes maximum incremental reactivity (Carter, 1994b).
3) MIR2 denotes maximum incremental reactivity (CARB, 2003).
4) MIR3 denotes maximum incremental reactivity (Carter, 2010a).
5) MIR4 denotes maximum incremental reactivity (Venecek, 2018).
6) ^aK denotes rate constant of NMHCs reaction with hydroxyl radicals at 298 K (Atkinson and Arey, 2003).

reaction with OH radical, and the impact of NO_3 radicals and some precipitation factors are negligible (Warneke et al., 2007). This may cause the initial mixing ratios to be lower than the actual mixing ratios.

2.3.2. Relative potential of NMHCs to evaluate ozone formation

There are various types of NMHCs, all of which have different photochemical reactivities and OFPs. The major indices that reflect the reactivities of NMHCs in photochemical processes and their contribution to ozone formation are the maximum incremental reactivity (MIR) factor and OH radical reactivity. OH radical reactivity is mainly calculated using the propylene-equivalent mixing ratio and the OH consumption rate (Darnall et al., 1976; Middleton et al., 1990). The evaluation of OH radical reactivity only considers the kinetic reactivity while neglecting the difference in the reaction mechanism and reactivity between peroxy radicals and NO. The photochemical reactivities of species that have a fast rate of reaction with OH radical are likely to be overestimated (Zou et al., 2019a,b). Although the assessment of the MIR factor also considers the kinetics, mechanism, and reactivity, the MIR factor itself is uncertain and is subject to different chemical mechanisms, local meteorological conditions, and atmospheric composition (e.g., Carter, 1994a; Carter, 1994b; Carb, 2003; Venecek et al., 2018; Mozaffar et al., 2020). The calculation of the MIR factor was initially based on the SAPRC-90 chemical mechanism (Carter, 1990; Carter, 1994a,b) and later based on the SAPRC-99 chemical mechanism (Carter, 2000; Carb, 2003). The most recently adopted chemical mechanism is SAPRC-07 (Carter, 2010a, b). All of these three MIR calculation methods were based on the 1988 standard scenario (meteorological parameters, emission rate, boundary layer height, and the VOC composition). Venecek et al., (2018) recently replaced the 1988 scenario with the 2010 scenario to recalculate the MIR factor.

To better compare and analyze the results, we used four MIR factor scales (Henceforth, MIR1 will refer to maximum incremental reactivity from Carter (1994b); MIR2 will refer to maximum incremental reactivity from Carb (2003); MIR3 will refer to maximum incremental reactivity from Carter (2010a); MIR4 will refer to maximum incremental reactivity from Venecek et al., (2018)) and the propylene-equivalent mixing ratio to calculate the chemical loss of NMHCs in the transport process and evaluated its impact on the OFP of NMHCs. The maximum ozone mixing ratio generated by NMHCs was calculated by multiplying the MIR values from four MIR scales (i.e., MIR1, MIR2, MIR3, and MIR4) (Carter, 1994b; Carb, 2003; Carter, 2010a; Venecek et al., 2018) (Table 2) with the actual volume mixing ratio of the corresponding NMHC species (Equation (3)). The propylene-equivalent mixing ratio (P) was obtained by normalization of the reactivity-weighted mixing ratio of OH radical. The reactivity-weighted mixing ratio of OH radical can be obtained by multiplying the carbon mixing ratio with the rate constant for the reaction of OH radical with NMHCs (K) (298 K, 1 standard atmosphere) (Equation (4)).

$$[\mathrm{NMHC}_i]_{\mathrm{MIR}} = \mathrm{MIR} \times [\mathrm{NMHC}_i] \times u_i/u_{\mathrm{ozone}} \quad (3)$$

Where u_i and u_{ozone} represent the relative molecular mass of NMHC species i and ozone, respectively, $[\mathrm{NMHC}_i]$ denotes the volume mixing ratio of NMHC species i, and $[\mathrm{NMHC}_i]_{\mathrm{MIR}}$ represents the maximum ozone mixing ratio that species i can generate. The relative OFPs of different NMHCs can be compared through the maximum ozone mixing ratio which different NMHCs can generate.

$$P_i = [\mathrm{NMHC}_i] \times \frac{K_i}{K_{\mathrm{C3H6}}} \quad (4)$$

Where P_i is the propylene-equivalent mixing ratio, $[\mathrm{NMHC}_i]$ represents the carbon mixing ratio of NMHC species i, and K_i and K_{C3H6} represent the rate constant for the reaction of OH radical with NMHC species i and the rate constant for the reaction of OH radical with propylene, respectively (Atkinson and Arey, 2003) (Table 2).

2.3.3. NMHCs source analysis

In this study, we used the PMF5.0 (positive matrix factorization) model developed by the US Environmental Protection Agency to analyze the sources of NMHCs. Based on the mass balance of the chemical substances between the observed mixing ratios and the source composition spectrum, the PMF treated the mixing ratio of a species j in a sample i (X_{ij}) observed as the contribution of the source region P. This mixing ratio is calculated by the following formula:

$$X_{ij} = \sum_{k=1}^{p} g_{ik} f_{kj} + e_{ij} \quad (5)$$

where X_{ij} is the mixing ratio of a species j in a sample i, g_{ik} is the contribution of source k to sample i, f_{kj} is the volume fraction of VOC species j in source k, p is the number of pollution sources, and e_{ij} is the residual error.

In the PMF model, the sum of the squares of the ratio of e_{ij} to the corresponding U_{ij} (uncertainty) of all samples is defined as the objective function Q, and the minimum solution of the objective function Q is solved to determine the composition spectrum and the contribution of the pollution source:

$$Q = \sum_{i=1}^{n} \sum_{j=1}^{m} \left[\frac{x_{ij} - \sum_{k=1}^{p} g_{ik} f_{kj}}{u_{ij}} \right]^2 \quad (6)$$

where m and n are the number of species and the number of samples, respectively, and U_{ij} is the uncertainty of species j in sample i. The PMF model settings are detailed by Guo et al., (2011).

3. Results and discussion

3.1. Estimation of initial NMHCs mixing ratios

As described in Section 2.3.1, the initial mixing ratios of NMHCs in the atmosphere are obtained by first estimating their chemical loss based on photochemical age. Since the reaction of NMHCs with OH radical at daytime is the major pathway of NMHCs oxidization and destruction (Atkinson and Arey, 2003), the initial mixing ratio of NMHCs in this study was only estimated at daytime (7:00–18:00). In this method, the age of the air mass is characterized by a group of specific NMHC species pairs with the same origin but with different chemical reactivities.

A critical step in the application of this method is the rational selection of species pairs. Firstly, when choosing the species pairs with obvious evidence of photochemical aging, the ratio of a reactive NMHCs (usually aromatics) to an inert NMHCs (e.g., ethyne) are used. Reductions of the ratios between selected aromatics and ethyne for the daytime samples (Table 3) show a clear evidence of photochemical aging and the selected aromatics (i.e., toluene (T), ethylbenzene (E), *m, p*-xylene (M,P) and o-xylene (O)) may be used as the species pairs in this study. Secondly, these aromatics with significant photochemical aging characteristics were selected for linear regression analysis to evaluate similarities in their emission source. As shown in Table 4, in summer and autumn, (E) had excellent linear relationships with (M, P) and with (O). Similarly, (M, P) had an excellent linear relationship with (O). The correlation coefficient (R^2) between (E) and (M, P), that between (E) and (O), and that between (M, P) and (O) were 0.95, 0.94, and 0.97, respectively, in summer, and 0.97, 0.96, and 0.97, respectively, in

Table 3
Ratios between selected aromatics to ethyne during summer and autumn.

Summer	T/e	E/e	M,P/e	O/e
Daytime	1.10	0.31	0.43	0.18
Nighttime	1.20	0.36	0.58	0.23
Autumn	T/e	E/e	M,P/e	O/e
Daytime	0.90	0.25	0.36	0.13
Nighttime	0.98	0.29	0.47	0.16

T: toluene; E: ethylbenzene; (M,P): m/p-xylene; O: o-xylene; e: ethyne.

Table 4
Correlation between selected aromatics during summer and autumn.

Summer	Toluene	Ethylbenzene	M/P-Xylene	O-Xylene
Toluene	1			
Ethylbenzene	0.75	1		
M/P-Xylene	0.73	0.95	1	
O-Xylene	0.71	0.94	0.97	1
Autumn	Toluene	Ethylbenzene	M/P-Xylene	O-Xylene
Toluene	1			
Ethylbenzene	0.87	1		
M/P-Xylene	0.82	0.97	1	
O-Xylene	0.81	0.96	0.97	1

autumn, indicating that the origins of these species pairs are consistent, although (T) was less correlated to the other species. (M, P) and (O) are not suitable to be used as species pairs, because they are isomers. As a result, species pair (E) and (M, P) and species pair (E) and (O) were selected in this study to calculate the initial mixing ratios of NMHCs.

An important parameter for the calculation is the ratio of emission between members of a species pair. Firstly, the selection of the initial emission ratio should take into account the influence of major emission sources in Guangzhou. Zheng et al., (2009) studied the emission inventory of VOCs in Guangzhou and found that plant emissions, vehicle emissions, and solvent consumption accounted for more than 80% of VOC emissions. Secondly, the selection of the initial emission ratio should refer to the characteristic ratio of the species in a particular emission process. Liu et al., (2008) showed that the initial emission ratio between E and (M, P) (henceforth, E/(M,P)) and that between (E) and (O) (henceforth, E/O) associated with vehicle emissions were approximately 0.3–0.5 and 0.7–1.0, respectively. Yuan et al., (2010) showed that the initial E/(M, P) and E/O associated with solvent consumption were approximately 0.4–0.5 and 1.4–1.6, respectively. Finally, the selection of the initial emission ratio in this study was also based on local measurements. The daytime variation patterns of E/(M, P), E/O, and O_x (NO_2+O_3) in summer and autumn suggested that they have a good consistency in time and intensity and that E/(M, P) and E/O well reflect the atmospheric photochemical ozone formation process of NMHCs (7:00–18:00) as shown in Fig. 3. The average E/(M, P) and E/O during the observation period (19:00 to 6:00 the next day) were used as the initial E/(M, P) and E/O. The calculated initial E/(M, P) was in 0.61 and 0.63, respectively, in summer and autumn. The calculated initial E/O was 1.55 and 1.60, respectively, in summer and autumn. In summary, we refer to the initial E/(M, P) in fresh plumes associated with vehicle emissions and solvent consumption, and the fresh plumes during the observation period. Based on this information, the initial emission ratios of E/(M, P) and E/O as used in the present study were set to 0.50 and 1.30, respectively.

Due to the importance of the initial emission ratio parameter, an assessment of the calculation's sensitivity to this parameter is necessary. The initial E/(M, P) of 0.3 and 0.7 and the initial E/O of 1.30 were used to examine this sensitivity and to make a comparison, respectively. The results showed that the relative variation range of the initial mixing ratios of NMHCs was 1.02–76.71% at the initial E/(M, P) of 0.3 and −0.67% to −39.92% at the initial E/(M, P) of 0.7. The relative variation range of the initial mixing ratios of NMHCs was 0.41–68.06% at the initial E/O of 1.3 when compared with the initial E/(M,P) of 0.5.

The estimation of the initial mixing ratios of NMHCs thereby greatly depends on the initial emission ratios for a given species pair, which is a cause of uncertainty in this assessment. In addition, the K_i (i.e., the rate constant for the reaction of OH radical with $NMHC_i$) used was according to Atkinson and Arey (2003) in Table 2, which assumes an average temperature of 298 K (24.85 °C). However, the measured daytime temperature varied 27.12°C–31.34 °C in summer and 22.37°C–28.30 °C in autumn. The assumption that the effect of temperature variations on K_i in summer and autumn could be ignored should be treated with some caution. Finally, according to de Gouw et al., (2005), when toluene (T)/benzene (B) and O/T were used to evaluate the rates of reaction between all major anthropogenic NMHC species and OH radical, the species removal rate was higher than that from using (T) alone and (O) alone, and the estimated initial mixing ratios became very unstable (such as those of alkenes). Therefore, for NMHC species with uniformly higher reaction rates than those of (M, P), their reaction rates were all set to the reaction rate of (M, P) in this study, which leads to an underestimation of the initial NMHCs mixing ratio.

3.2. Observed and initial NMHCs composition characterization

Fig. 4 shows the mixing ratios of \four categories of NMHCs for the daytime observed (Obs-D), daytime initial (Ini-D), and nighttime observed (Obs-N) as well as their relative contributions (%) during the summer and autumn at GPACS. Alkanes presented the largest contribution to the total daytime observed and initial NMHCs mixing ratios in both, summer and autumn. Alkenes had a larger contribution to total initial daytime NMHCs mixing ratio than that of aromatics in summer, while the opposite was observed during autumn. This phenomenon occurred mainly because the mixing ratio of isoprene (one of the major components of alkenes) from biogenic emission in summer was higher than that in autumn owing to the higher temperature and higher levels of solar radiation in summer. Alkynes provided the smallest contributions. By initial mixing ratio estimation (see Section 3.1 for details on calculation), we found that the initial daytime mixing ratios in summer and autumn were 37.30 ppbv and 41.62 ppbv, respectively, which were 6.90 ppbv and 5.98 ppbv higher than the observed mixing ratios. The differences between the initial daytime mixing ratios and observed mixing ratios in this study are lower than those in previous studies in Beijing (7.72 ppbv) (Gao et al., 2018) and Shanghai (9.60 ppbv) (Wang et al., 2013). The initial mixing ratios of alkenes in summer and autumn were higher than the observed mixing ratios of alkenes by 3.20 ppbv and 2.23 ppbv, respectively, which are the largest differences between initial

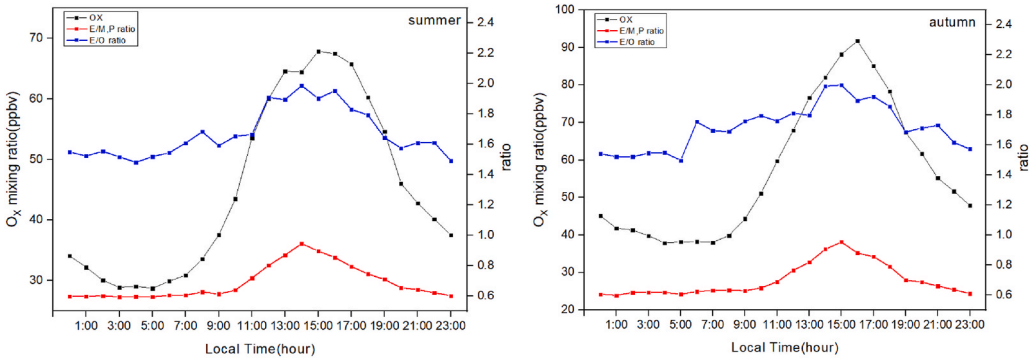

Fig. 3. Diurnal variation of Ox, E/X and E/O during summer (left) and autumn (right) at GPACS.

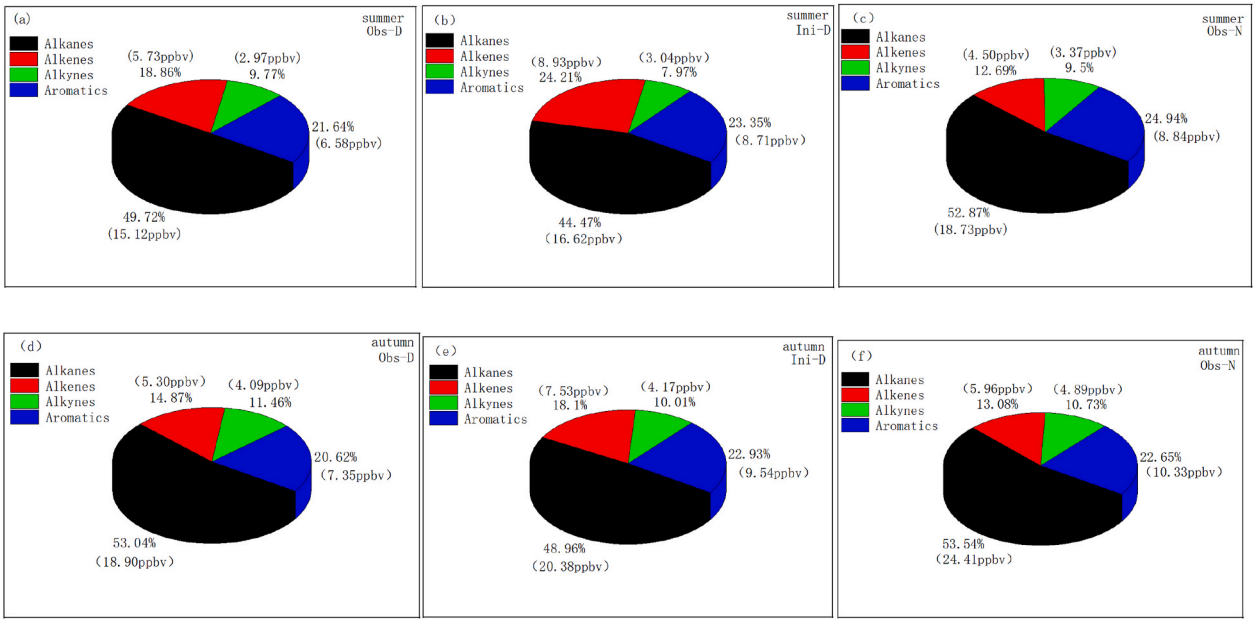

Fig. 4. The mixing ratios (ppbv) and relative contributions (%) of four categories of NMHCs for the daytime observed (Obs-D), daytime initial (Ini-D), and nighttime observed (Obs-N) during the summer (figures a, b, and c) and autumn (figures d, e, and f) at GPACS.

daytime mixing ratios and observed mixing ratios among the NMHC components. Alkenes also had the largest increase in the relative contributions of chemical mixing ratio loss (initial daytime minus observed daytime) in summer (5.35%) and autumn (3.23%). This result indicates that the chemical reactivity of alkenes is very strong, and the rate of reaction of alkenes with OH radical is fast, resulting in a high consumption of alkenes during the daytime. Aromatics also showed strong chemical reactivity. The initial mixing ratios of aromatics in summer and autumn were higher than the observed mixing ratios by 2.13 ppbv and 2.19 ppbv, respectively. The relative contributions of the chemical mixing ratio loss for aromatics in summer and autumn increased by 1.71% and 2.31%, respectively. However, the relative contributions of the chemical mixing ratio loss for alkanes and alkynes decreased in summer and autumn. The observed daytime mixing ratios of NMHCs were lower than the nighttime mixing ratios by 5.04 ppbv and 9.95 ppbv in summer and autumn, respectively. Although NMHCs emissions associated with oil or solvent volatilization are more intense in daytime than at night (Zou et al., 2019b), this phenomenon occurred mainly because of the lower temperature and boundary layer height at nighttime are more conducive to pollutant accumulation and because NMHCs are more prone to photochemical loss under intense daylight.

3.3. Ozone formation potential

As mentioned in section 2.3.2, the uncertainty of the MIR factor varies with different chemical mechanisms, local meteorological conditions, and atmospheric composition. For this reason, four MIR factor scales (MIR1, MIR2, MIR3, and MIR4) were used to evaluate the OFP based on the initial daytime mixing ratios and the observed daytime mixing ratios of NMHCs in summer and autumn (as shown in Table 5). We found that the OFP based on NMHC loss in summer and autumn were 62.67 ppbv, 73.05 ppbv, 73.31 ppbv, 68.51 ppbv and 47.71 ppbv, 55.54 ppbv, 56.12 ppbv, 52.68 ppbv, respectively. The results show that the OFP estimated using the MIR factor scale (Carter, 1994) were significantly lower than those estimated using other MIR factor scales. This is likely because some NMHCs (such as 2,2-dimethylbutane, o-ethyltoluene, m-ethyltoluene, p-ethyltoluene, m-diethylbenzene and p-diethylbenzene) were not included in the early research (Table 2). In addition, the MIR factor is constrained by various chemical mechanisms, local meteorological conditions, and atmospheric composition. For example, the results of this study found that OFP estimated using the 1988 scenario-based MIR (Carter, 2010) was lower than that estimated using the 2010 scenario-based MIR (Venecek, 2018). Specifically, the OFP based on initial (observed) mixing ratios using the MIR (Carter, 2010) were smaller than those using the MIR (Venecek, 2018) by 3.65% (2.20%) during summer and 2.69% (1.35%) during autumn. In addition, there were some minor changes in the proportions of different components. In summer, the initial daytime mixing ratios of alkanes, alkenes, alkynes, and aromatics varied by 2.9%, 2.14%, 0.02%, and 0.79%, respectively, and the observed daytime mixing ratios of alkanes, alkenes, alkynes, and aromatics varied by 3.39%, 2.4%, 0.01%, and 1.01%. In autumn, the initial daytime mixing ratios of alkanes, alkenes, alkynes, and aromatics varied by 3.03%, 1.7%, 0.02%, and 1.36%, respectively, and the observed daytime mixing ratios of alkanes, alkenes, alkynes, and aromatics varied by 3.38%, 1.84%, 0.01%, and 1.55% (as shown in Fig. 5).

Nevertheless, the relative rankings of NMHC species that made large contributions to ozone formation were essentially the same according to the two MIR factor scales (Carter, 2010 and Venecek, 2018) (as shown in Table 6), indicating that the OFP assessed using the previously adopted MIR factor (Carter, 2010) still possess certain reference value for the formulation of ozone prevention and control measures. NMHC species that make large contributions to ozone formation (such as isoprene, *m*, *p* -xylene, and toluene) should be preferentially controlled. In addition,

Table 5
The OFP calculated using observed daytime (Obs-D) and initial daytime (Ini-D) mixing ratio based on the method of four MIR factor scales during summer and autumn at GPACS.

Summer	MIR1	MIR2	MIR3	MIR4
Ini-D (ppbv)	199.01	238.45	236.26	227.95
Obs-D (ppbv)	136.34	165.40	162.95	159.44
Autumn	MIR1	MIR2	MIR3	MIR4
Ini-D (ppbv)	175.21	212.20	210.54	205.03
Obs-D (ppbv)	127.50	156.66	154.42	152.35

1) MIR1 denotes maximum incremental reactivity (Carter, 1994b).
2) MIR2 denotes maximum incremental reactivity (CARB, 2003).
3) MIR3 denotes maximum incremental reactivity (Carter, 2010a).
4) MIR4 denotes maximum incremental reactivity (Venecek, 2018).

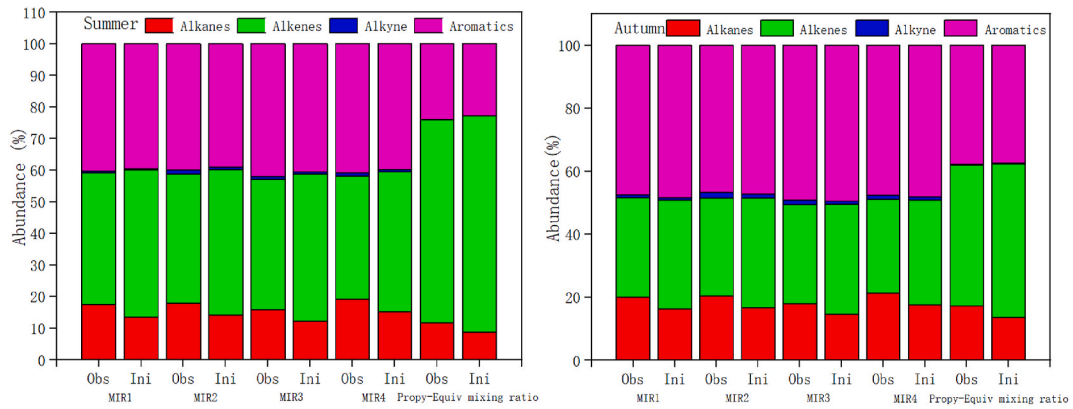

Fig. 5. The OFP abundance of different components estimated using observed (Obs) and initial (Ini) mixing ratio based on the method of the MIR (MIR1 (Carter, 1994b), MIR2 (CARB, 2003), MIR3 (Carter, 2010), MIR4 (Venecek, 2018)) and Propy-Equiv scales during summer (left) and autumn (right) during the daytime at GPACS.

Table 6
Relative contributions to ozone formation based on initial mixing ratios by the top 10 NMHC species using the MIR methods and Propy-Equiv scales during the summer and autumn at GPACS.

MIR1 Summer		MIR2 Summer		MIR3 Summer		MIR4 Summer		Propy-Equiv Summer	
Compound	%	Compound	%	Compound	%	Compound	%	Compound	%
Isoprene	30.1	Isoprene	29.6	Isoprene	29.6	Isoprene	28.1	Isoprene	56.9
m,p-Xylene	17.9	m,p-Xylene	15.0	m,p-Xylene	15.9	m,p-Xylene	14.8	m,p-Xylene	8.7
Toluene	9.9	Toluene	11.9	Toluene	12.3	Toluene	12.9	cis-2-Pentene	6.9
cis-2-Pentene	5.6	cis-2-Pentene	5.5	cis-2-Pentene	5.6	cis-2-Pentene	5.4	Styrene	4.7
o-Xylene	5.5	o-Xylene	5.3	o-Xylene	5.4	o-Xylene	5.3	Toluene	3.8
Ethene	4.4	Ethene	4.5	Ethene	4.5	Ethene	4.4	o-Xylene	2.0
Propene	3.7	Propene	3.8	Propene	3.9	Propene	3.7	Cyclohexane	1.8
Ethylbenzene	3.3	Ethylbenzene	2.8	Ethylbenzene	3.1	Ethylbenzene	3.3	Propene	1.7
Cyclohexane	1.9	Cyclohexane	1.8	Cyclohexane	1.5	Cyclohexane	2.3	Ethylbenzene	1.5
i-Pentane	1.7	i-Pentane	1.8	i-Pentane	1.5	i-Pentane	1.8	n-Hexane	0.8
MIR1 Autumn		MIR2 Autumn		MIR3 Autumn		MIR4 Autumn		Propy-Equiv Autumn	
Compound	%	Compound	%	Compound	%	Compound	%	Compound	%
m,p-Xylene	22.6	m,p-Xylene	18.8	m,p-Xylene	19.8	m,p-Xylene	18.3	Isoprene	34.2
Isoprene	13.3	Toluene	15.0	Toluene	15.5	Toluene	16.0	m,p-Xylene	14.9
Toluene	12.6	Isoprene	12.9	Isoprene	12.9	Isoprene	12.1	Styrene	7.2
Ethene	8.0	Ethene	8.1	Ethene	8.1	Ethene	8.0	Toluene	6.7
Propene	7.1	Propene	7.2	Propene	7.3	Propene	6.9	Propene	4.4
o-Xylene	5.9	o-Xylene	5.6	o-Xylene	5.8	o-Xylene	5.5	cis-2-Pentene	4.0
Ethylbenzene	4.1	Ethylbenzene	3.5	Ethylbenzene	3.9	Ethylbenzene	4.1	o-Xylene	3.0
cis-2-Pentene	2.4	cis-2-Pentene	2.3	cis-2-Pentene	2.4	cis-2-Pentene	2.3	Ethylbenzene	2.5
i-Pentane	2.0	n-Butane	2.1	n-Butane	1.8	n-Butane	2.2	Ethene	2.1
n-Butane	2.0	i-Pentane	2.0	i-Pentane	1.7	i-Pentane	2.0	Cyclohexane	1.8

1) MIR1 denotes maximum incremental reactivity (Carter, 1994b).
2) MIR2 denotes maximum incremental reactivity (CARB, 2003).
3) MIR3 denotes maximum incremental reactivity (Carter, 2010a).
4) MIR4 denotes maximum incremental reactivity (Venecek, 2018).

the OFP based on initial daytime mixing ratios using the propylene-equivalent mixing ratio accounted for: alkanes: 8.68% (13.52%), alkenes: 68.52% (48.83%), alkynes: 0.12% (0.26%), and aromatics: 22.68% (37.39%), in summer (autumn), respectively.

The OFP based on the observed daytime mixing ratios of alkanes, alkenes, alkynes, and aromatics assessed using the propylene-equivalent mixing ratio accounted for 11.79%, 64.20%, 0.19%, and 23.82%, respectively, in summer and 17.39%, 44.52%, 0.37%, and 37.72% in autumn. Since the assessment method using propylene-equivalent mixing ratio only considers the kinetic reactivity and ignores the differences in the mechanism and reactivity of the reaction between peroxy radicals and NO, the OFP of the species with a fast OH radical reaction rate assessed with this method might be overestimated, resulting in an overestimated proportion of alkenes. According to Table 6, eight species in summer were among the top 10 species in autumn. However, their rankings in summer differed from those in autumn. This finding indicates that both methods can reflect the reactivity and OFP of each NMHC species to some extent. In particular, the two methods have high consistency in describing the species that contribute the most to ozone formation.

3.4. Source apportionment

Since NMHCs undergo photochemical loss during transport, the emission sources can be better reflected by source analysis based on initial mixing ratios. The PMF5.0 model was used in this study to analyze the sources of atmospheric NMHCs in Guangzhou based on the initial mixing ratios of NMHCs. Benzene was excluded from the source analysis

in this study due to its abnormal mixing ratios.

Based on the principle that each source has a tracer species and that the tracers representing the sources of different NMHCs are not assigned to the same factor, a total of six potential NMHC sources were revealed by the PMF model. Fig. 6 shows these NMHC sources: vehicle emissions, liquefied petroleum gas (LPG) usage, gasoline evaporation, paint & varnish, consumer & household products, and biogenic volatile organic compounds (BVOCs). In factor 1, tracers of vehicle emissions, such as ethane, ethene, and acetylene account for a high proportion (53.6%) of NMHCs and are accompanied by a high proportion of aromatics. The similarity between the source spectrum and the NMHC composition of vehicle emissions is high (Guo et al., 2004). Therefore, this factor represents vehicle emissions. In factor 2, propane, *n*-butane and *i*-butane accounted for a significant proportion (52.8%), and all three NMHCs are typical LPG components. Therefore, factor 2 reflects LPG vehicle emissions or LPG usage (Guo et al., 2004, 2007). In factor 3, *n*-pentane accounted for the highest proportion (37.7%), followed by *i*-pentane (31.8%), which is related to gasoline vehicle emissions. However, the contents of short-chain alkenes and toluene were low in this factor. Therefore, this factor may be related to gasoline volatilization. In factor 4, higher mixing ratios of toluene, ethylbenzene, and xylene were found, accompanied by large amounts of 3-methylhexane and *n*-heptane. Therefore, factor 4 may be related to solvent consumption, such as in paint and varnish (Lyu et al., 2016). In factor 5, there were higher mixing ratios of 2-/3-methylphenane and *n*-hexane. *n*-Hexane and *i*-hexane are commonly used solvents in industries, such as extraction and synthetic rubber production. Therefore, this factor was identified as industrial solvent consumption (An et al., 2014; Lash and Parker, 2001). In factor 6, isoprene accounted for the highest proportion. Therefore, this factor was a typical BVOC source.

Based on NMHCs loadings in each source diagnosed from PMF model, Fig. 7 summarizes the percentage contributions of the source to NMHCs in summer and autumn. In terms of the contributions of various industries, the differences between summer and autumn were not significant. In general, vehicle exhaust emissions were an important source of NMHCs in Guangzhou, accounting for 34% in summer and 33% and in autumn. In the fuel industry associated with LPG usage and gasoline evaporation accounted for 24–27%. Solvent consumption was also an important source of NMHCs in Guangzhou, in which paint and varnish accounted for 18–19% and industrial solvents accounted for 10–17%.

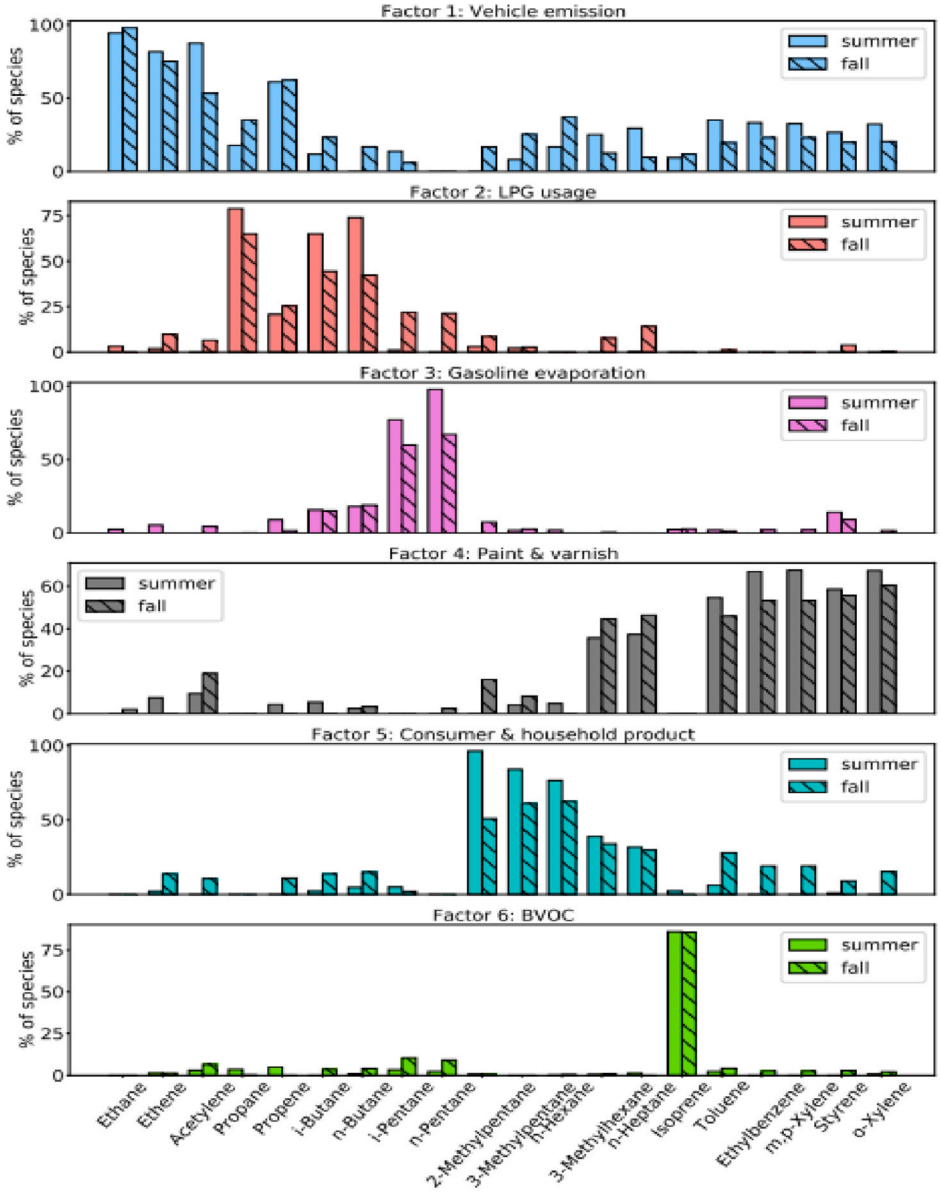

Fig. 6. Main sources of NMHCs in ambient air and the contributions of individual compounds at GPACS.

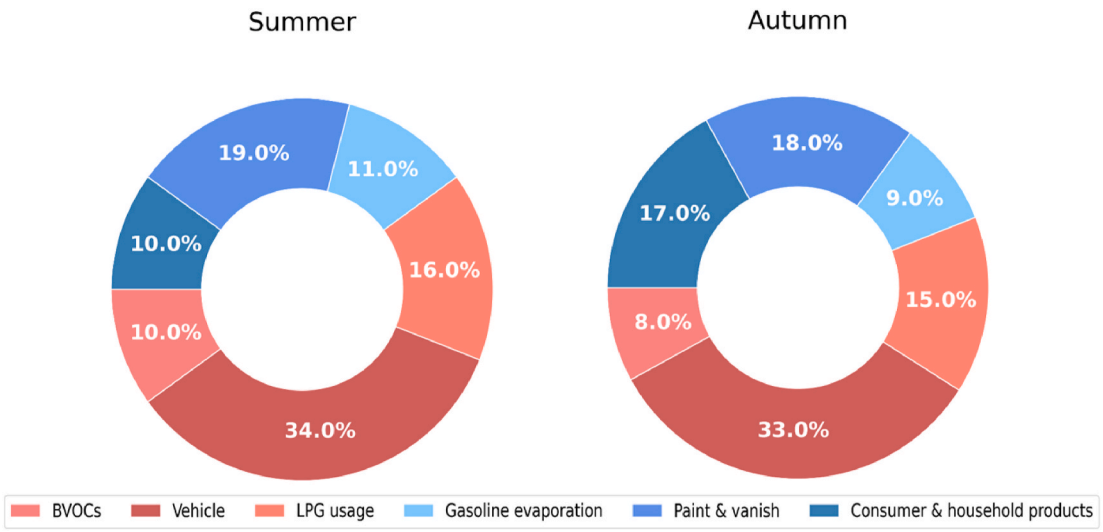

Fig. 7. NMHCs emission contributions (%) during summer and autumn at GPACS.

There was no significant difference between BVOCs in summer and autumn, BVOCs accounting for 10% in summer and 8% in autumn (as shown in Fig. 7).

4. Conclusions

In this study, the chemical loss of 55 non-methane hydrocarbons (NMHCs) was estimated using the photochemical age-based method on the online observation data of the NMHCs in summer (June, July, and August) and autumn (September, October, and November) 2012 at the Guangzhou Panyu Atmospheric Composition Station (GPACS) in the Pearl River Delta (PRD). Subsequently, the composition characteristics, ozone formation potential (OFP), and potential sources of the NMHCs were analyzed under the condition of atmospheric photochemical loss to provide a guideline for the comprehensive management of atmospheric photochemical ozone in Guangzhou.

The results showed that the initial mixing ratios of NMHCs during summer and autumn were 37.30 ppbv and 41.62 ppbv, which were 6.90 ppbv and 5.98 ppbv higher than the observed mixing ratios, respectively. Alkenes have strong chemical reactivity and a high reaction rate with OH radical, resulting in a high depletion of alkenes during the daytime.

Four maximum incremental reactivity (MIR) scales were used to evaluate the OFP based on initial daytime mixing ratios and observed daytime mixing ratios of NMHCs in summer and autumn. The obtained OFPs were 62.67 ppbv, 73.05 ppbv, 73.31 ppbv, and 68.51 ppbv in summer and 47.71 ppbv, 55.54 ppbv, 56.12 ppbv, and 52.68 ppbv in autumn as calculated by the respective MIR scales. Eight species evaluated by MIR were among the top 10 species assessed by propylene-equivalent mixing ratio, although their rankings differed. This indicates that both MIR and propylene-equivalent mixing ratio method can reflect the reactivities and OFPs of various NMHC species to a certain extent. NMHC species that contributed most to ozone formation (such as isoprene, m, p -xylene, and toluene) should be preferentially controlled.

Source analysis using positive matrix factorization (PMF) based on initial NMHC mixing ratios revealed that the contributions of various industries were similar between summer and autumn. Vehicle emissions and solvent consumption were the major sources of NMHCs in Guangzhou.

Since the results presented in this work are based on NMHCs mixing ratios, further investigation using a wider variety of VOCs species (e.g., OVOCs) is needed to obtain more detailed and robust conclusions.

CRediT authorship contribution statement

Y. Zou: Conceptualization, Methodology, Software, Formal analysis, Investigation, Writing – original draft, Visualization, Writing – review & editing. **E. Charlesworth:** Writing – review & editing. **N. Wang:** Methodology, Formal analysis, Software, Writing – review & editing. **R. M. Flores:** Writing – review & editing. **Q.Q. Liu:** Writing – review & editing. **F. Li:** Writing – review & editing. **T. Deng:** Writing – review & editing. **X.J. Deng:** Writing – review & editing.

Declaration of competing interest

The authors declare that they have no known competing financial interests or personal relationships that could have appeared to influence the work reported in this paper.

Acknowledgements

This work was supported by the National Natural Science Foundation of China (41905123, 41805131), Guangdong Basic and Applied Basic Research Foundation (2020A1515011136,2019A1515110791), Key-Area Research and Development Program of Guangdong Province (2020B1111360003), National Key Research and Development Program of China (2018YFC0213901, 2019YFC0214605, 2016YFC0203305), Science and Technology Research project of Guangdong Meteorological Bureau (GRMC2018M06, GRMC2018M07) and Science and Technology Innovation Team Plan of Guangdong Meteorological Bureau (GRMCTD202003).

References

An, J.L., Zhu, B., Wang, H.L., et al., 2014. Characteristics and source apportionment of VOCs measured in an industrial area of Nanjing, Yangtze River Delta, China. Atmospheric Environment 97, 206–214.

Atkinson, R., Arey, J., 2003. Atmospheric degradation of volatile organic compounds. Chem. Rev. 103, 4605–4638.

Bertman, S.B., Roberts, J.M., Parrish, D.D., et al., 1995. Evolution of alkyl nitrates with air mass age. Journal of Geophysical Research Atmosphere 100 (D11), 22805–22814.

Bon, D.M., Ulbrich, I.M., de Gouw, J.A., et al., 2011. Measurements of volatile organic compounds at a suburban ground site(T1) in Mexico City during the MILAGRO 2006 campaign: measurement comparison, emission ratios, and source attribution. Atmos. Chem. Phys. 11 (6), 2399–2421.

CARB, 2003. Rulemaking on the adoption of proposed amendments to the tables of maximum incremental reactivity (MIR) values, California air resources board, December 3. Available at. http://www.arb.ca.gov/regact/mir2003/mir2003.htm. http://www.arb.ca.gov/regact/mir2003/fsor.doc. Accessed August 14, 2009. Document giving MIR values is available at:

Carter, W.P.L., 1994a. Calculation of Reactivity Scales Using an Updated Carbon Bond IV Mechanism, Report Prepared for Systems Applications Internation for the Auto/Oil Air Quality Improvement Program.
Carter, W.P.L., 1994b. Development of ozone reactivity scales for volatile organic compounds. J. Air Waste Manag. Assoc. 44 (7), 881–899.
Carter, W.P.L., 2010a. Development of the SAPRC-07 chemical mechanism and updated ozone reactivity scales," final report to the California air resources board Contract No. 03-318. January 27. Available at: www.cert.ucr.edu/~carter/SAPRC.
Carter, W.P.L., 2010b. Development of the SAPRC-07 chemical mechanism. Atmos. Environ. 44 (40), 5324–5335.
Cheng, H.R., Guo, H., Saunders, S.M., et al., 2010. Roles of volatile organic compounds in photochemical ozone formation in the atmosphere of the Pearl River Delta, southern China. Air Quality and Climate Change 44 (4), 29–38.
Darnall, K.R., Lloyd, A.C., Winer, A.M., et al., 1976. Reactivity scale for atmospheric hydrocarbons based on reaction with hydroxyl radical. Environ. Sci. Technol. 10, 692–696.
de Gouw, J.A., Middlebrook, A.M., Warneke, C., 2005. Budget of organic carbon in a polluted atmosphere: results from the New England air quality study in 2002. Journal of Geophysical Research Atmosphere 110. D16305.
Gao, J., Zhang, J., Li, H., et al., 2018. Comparative study of volatile organic compounds in ambient air using observed mixing ratios and initial mixing ratios taking chemical loss into account-A case study in a typical urban area in Beijing. Sci. Total Environ. 628–629, 791–804.
Guo, H., Wang, T., Louie, P.K.K., 2004. Source apportionment of ambient non-methane hydrocarbons in Hong Kong: application of a principal component analysis/absolute principal component scores (PCA/APCS) receptor model. Environ. Pollut. 129, 489–498.
Guo, H., So, K.L., Simpson, I.J., et al., 2007. C_1-C_8 volatile organic compounds in the atmosphere of Hong Kong: overview of atmospheric processing and source apportionment. Atmos. Environ. 41, 1456–1472.
Guo, H., Cheng, H.R., Ling, Z.H., et al., 2011. Which emission sources are responsible for the volatile organic compounds in the atmosphere of Pearl River Delta? J. Hazard Mater. 188, 116–124.
Guo, H., Ling, Z.H., Cheng, H.R., et al., 2017. Tropospheric volatile organic compounds in China. Sci. Total Environ. 574, 1021–1043.
Lash, L.H., Parker, J.C., 2001. Hepatic and renal toxicities associated with perchloroethylene. Pharmacol. Rev. 53, 177–208.
Ling, Z.H., Zhao, J., Fan, S.J., et al., 2017. Sources of formaldehyde and their contributions to photochemical O3 formation at an urban site in the Pearl River Delta, southern China. Chemosphere 168, 1293–1301.
Liu, Y., Shao, M., Fu, L.L., et al., 2008. Source profiles of volatile organic compounds (VOCs) measured in China: part I. Atmos. Environ. 42, 6247–6260.
Liu, L., Tan, H.B., Fan, S.J., et al., 2018. Influence of aerosol hygroscopicity and mixing state on aerosol optical properties in the Pearl River Delta region, China. Sci. Total Environ. 627, 1560–1571.
Lyu, X.P., Chen, N., Guo, H., et al., 2016. Ambient volatile organic compounds and their effect on ozone production in Wuhan, central China. Sci. Total Environ. 541, 200–209.
Main, H.H., Roberts, P.T., Hurwitt, S.B., 1999. Validation of PAMS VOC Data in the Mid-Atlantic Region. Report Prepared for MARAMA, Baltimore, MD. Sonoma Technology,Inc., Petaluma, CA STI-998481-1835-FR.
McKeen, S.A., Liu, S.C., Hsie, E.Y., et al., 1996. Hydrocarbon ratios during PEM-WEST A: a model perspective. J. Geophys. Res. 101, 2087–2109.
Middleton, P., Stockwell, W.R., Carter, W.P.L., 1990. Aggregation analysis of volatile organic compound emissions for regional modeling. Atmos. Environ. 24A, 1107–1133.
Mozaffar, A., Zhang, Y., Fan, M., et al., 2020. Characteristics of summertime ambient VOCs and their contributions to O_3 and SOA formation in a suburban area of Nanjing, China. Atmos. Res. 240, 104923.
Na, K., Kim, Y.P., 2007. Chemical mass balance receptor model applied to ambient C_2-C_9 VOC concentration in Seoul, Korea: effect of chemical reaction losses. Atmos. Environ. 41, 6715–6728.
Ou, J.M., Yuan, Z.B., Zheng, J.Y., et al., 2016. Ambient ozone control in a photochemically active region: short-term despiking or long-term attainment? Environ. Sci. Technol. 50, 5720–5728.
Parrish, D.D., Stohl, A., Forster, C., et al., 2007. The effects of mixing on evolution of hydrocarbon ratios in the troposphere. Journal of Geophysical Research Atmosphere 112, D10S34.
Shao, M., Zhao, M.P., Zhang, Y.H., et al., 2000. Biogenic VOCs emissions and its impact on ozone formation in major cities of China. Journal of Environmental Science and Health, Part A 35 (10), 1941–1950.
Shao, M., Wang, B., Lu, S.H., et al., 2011. Effects of Beijing Olympic control measures of reducing reactive hydrocarbon species. Environ. Sci. Technol. 45, 514–519.
Shiu, C.J., Liu, S.C., Chang, C.C., et al., 2007. Photochemical production of ozone and control strategy for Southern Taiwan. Atmos. Environ. 41, 9324–9340.
Tan, H.B., Liu, L., Fan, S.J., et al., 2016. Aerosol optical properties and mixing state of black carbon in the Pearl River Delta, China. Atmos. Environ. 131, 196–208.
Venecek, M.A., Carter, W.P.L., Kleeman, M.J., 2018. Updating the SAPRC maximum incremental reactivity (MIR) scale for the United States from 1988 to 2010. J. Air Waste Manag. Assoc. 2162–2906.
Wang, T., Wei, X.L., Ding, A.J., et al., 2009. Increasing surface ozone concentrations in the background atmosphere of Southern China, 1994-2007. Atmos. Chem. Phys. 9, 6217–6227.
Wang, H.L., Chen, C.H., Wang, Q., et al., 2013. Chemical loss of volatile organic compounds and its impact on the source analysis through a two-year continuous measurement. Atmos. Environ. 80, 488–498.
Wang, N., Lyu, X., Deng, X., et al., 2019. Aggravating O_3 pollution due to NOx emission control in eastern China. Sci. Total Environ. 677, 732–744.
Warneke, C., Mckeen, S.A., de Gouw, J.A., et al., 2007. Determination of urban volatile organic compound emission ratios and comparison with an emissions database. Journal of Geophysical Research Atmosphere 112, D10S47.
Wiedinmeyer, C., Friedfeld, S., Baugh, W., et al., 2001. Measurement and analysis of atmospheric concentrations of isoprene and its reaction products in central Texas. Atmos. Environ. 35 (6), 1001–1013.
Xie, X., Shao, M., Liu, Y., et al., 2008. Estimate of initial isoprene contribution to ozone formation potential in Beijing, China. Atmos. Environ. 42, 6000–6010.
Yuan, B., Shao, M., Lu, S.H., et al., 2010. Source profiles of volatile organic compounds associated with solvent use in Beijing, China. Atmos. Environ. 44, 1919–1926.
Zhan, J.L., Feng, Z.M., Liu, P.F., et al., 2021. Ozone and SOA formation potential based on photochemical loss of VOCs during the Beijing summer. Environ. Pollut. 285 https://doi.org/10.1016/j.envpol.2021.117444.
Zhang, Y.H., Su, H., Zhong, L.J., et al., 2008. Regional ozone pollution and observation-based approach for analyzing ozone-precursor relationship during the PRIDEPRD2004 campaign. Atmos. Environ. 42, 6203–6218.
Zheng, J.Y., Shao, M., Che, W.W., et al., 2009. Speciated VOC emission inventory and spatial patterns of ozone formation potential in the Pearl River Delta, China. Environ. Sci. Technol. 43 (22), 8580–8586.
Zheng, J.Y., Zhong, L.J., Wang, T., et al., 2010. Ground-level ozone in the Pearl River Delta region: analysis of data from a recently established regional air quality monitoring network. Atmos. Environ. 44, 814–823.
Zou, Y., Deng, X.J., Zhu, D., et al., 2015. Characteristics of 1 year of observational data of VOCs, NOx and O3 at a suburban site in Guangzhou, China. Atmos. Chem. Phys. 15, 6625–6636.
Zou, Y., Charlesworth, E., Yin, C.Q., et al., 2019a. The weekday/weekend ozone differences induced by the emissions change during summer and autumn in Guangzhou, China. Atmos. Environ. 199, 114–126.
Zou, Y., Deng, X.J., Deng, T., et al., 2019b. One-year characterization and reactivity of isoprene and its impact on surface ozone formation at a suburban site in Guangzhou, China. Atmosphere 10, 201. https://doi.org/10.3390/atmos10040201.